Colloid Polym Sci 276:197–205 (1998)

ORIGINAL CONTRIBUTION

J.F. Widmann
C.M. Heusmann
E. James Davis

The effect of a polymeric additive on the evaporation of organic aerocolloidal droplets

Received: 17 June 1997
Accepted: 24 October 1997

J.F. Widmann[1] · C.M. Heusmann
E. James Davis (✉)
Department of Chemical Engineering
Box 351750
University of Washington
Seattle, WA 98195-1750
USA

[1]*Current address*
National Institute of Standards
and Technology
High Témperature Processes Group
Bldg. 221, Rm. B312
Gaithersburg, MD 20899
USA

Abstract The evaporation of single triethyl phosphate (TEP) microdroplets containing a high molecular weight polymer, poly(methyl methacrylate) (PMAA), was investigated using an electrodynamic trap and light scattering measurements to explore the suppression of evaporation by the additive. Pure-component evaporation rates were measured to determine the vapor pressure over a range of temperatures, and the polymer was found to significantly decrease the evaporation rate. A numerical solution of the problem of simultaneous solvent evaporation and polymer diffusion within the droplet indicated a rapid build-up of PMMA at the surface of the drop, but vapor/liquid thermodynamic considerations alone do not account for the observed reduction in the evaporation rate for the droplets containing PMMA. After significant evaporation of TEP occurred, the ultra-low evaporation rate was measured using changes in the Raman spectra associated with morphology-dependent resonances. The evaporation in this regime appears to be controlled by the rate of solvent molecules diffusing through the polymer matrix.

Key words Microdroplets – polymer solutions – triethyl phosphate – poly(methyl methacrylate) – electrodynamic balance

Introduction

A variety of additives are used to alter the properties of fuels. In this study we examined the use of high molecular weight polymer to reduce the evaporation rate of the oxygenated compound, triethyl phosphate. The use of levitation techniques to study the chemistry and physics of single aerosol particles has been extensive since the classic experiments in which Millikan [1] measured the charge on the electron by suspending oil drops electrostatically. The electrodynamic balance (EDB), an outgrowth of the Millikan apparatus, permits the investigation of single microparticles, eliminating the complicating effects of polydispersity, particle–particle interactions, and particle–container interactions. Davis [2] recently reviewed the history of microparticle levitation and its applications, including investigations of light scattering, evaporation, condensation, chemical reactions, phase transitions, highly concentrated solution thermodynamics, and phoretic forces.

A number of investigators have used the electrodynamic balance to measure the evaporation rate of organic microdroplets. Taflin et al. [3] monitored the size change of droplets composed of several different organics using elastic light scattering measurements. Rubel [4] studied the evaporation of multicomponent fuel droplets consisting of a high-boiling petroleum fraction (100 pale oil), and Ravindran and Davis [5] measured the size change of submicrometer binary droplets composed of dioctyl phthalate and dibutyl phthalate. Rubel [6] later reported evaporation rates for that same binary system using droplets an order of magnitude larger. Rubel and

Milham [7] obtained "effective" vapor pressures of 100 pale oil by modeling the droplet as consisting of 15 "components" and assuming ideal behavior.

By analyzing binary pairs selected from the chemicals 1-bromododecane, 1,8-dibromooctane, hexadecane, and heptadecane, Allen et al. [8] determined activity coefficients for the mixtures. Buehler et al. [9] used Raman spectroscopy to monitor the evaporation of binary component aerosols, following the distillation of droplets containing 1,8-dibromooctane and hexadecane by recording the intensity of the Raman peak corresponding to the C–Br bond in dibromooctane. Aardahl et al. [10] used a combination of elastic and inelastic light scattering to follow the evaporation of levitated droplets composed of 1-iododecane and 1-bromotetradecane, both of which have Raman-active carbon–halogen bonds. Recently, Widmann and Davis [11] reported evaporation rates for droplets composed of four and five components. They found that the data were in good agreement with a theoretical analysis based upon the UNIFAC model for liquid-phase activity coefficients.

The prior studies indicate that multicomponent evaporation rates can be predicted for systems containing relatively low molecular weight compounds, but the presence of high molecular weight components complicates the evaporation process. This paper explores the effect of the polymer additive, poly(methyl methacrylate) (PMMA), on the evaporation rate of organic aerosols composed of triethyl phosphate (TEP).

Theory

Diffusion controlled evaporation

At ambient temperature and pressure, the evaporation of a liquid droplet well below its boiling point is controlled by diffusion of vapor into the surrounding gas. For evaporation of a single volatile component A into carrier gas G, the evaporation process was analyzed by Maxwell [12]. For quasi-steady state evaporation he obtained

$$\frac{\mathrm{d}m_\mathrm{A}}{\mathrm{d}t} = -\frac{4\pi a D_\mathrm{AG} M_\mathrm{A}}{R}\left[\frac{p^0_\mathrm{A}(T_a)}{T_a} - \frac{P^\infty_\mathrm{A}(T_\infty)}{T_\infty}\right], \tag{1}$$

where m_A is the mass of the drop, a is the drop radius, D_AG is the diffusion coefficient of the vapor, A, having molecular weight M_A, in stagnant gas, G. The temperature at the surface of the drop is T_a, R is the gas constant, $p^0_\mathrm{A}(T_a)$ is the vapor pressure of the liquid at temperature T_a, and $p^\infty_\mathrm{A}(T_\infty)$ is the partial pressure of vapor in the bulk gas at temperature T_∞.

For a slowly evaporating drop of density ρ_L the evaporation proceeds isothermally, and Eq. (1) can be integrated to give

$$a^2 = a_0^2 - S_\mathrm{AG}(t - t_0)\,, \tag{2}$$

where a_0 is the radius at time t_0. From Eq. (2), a plot of a^2 versus time should yield a straight line. The slope, $-S_\mathrm{AG}$, depends only on the material properties, temperature, vapor pressure, and gas-phase diffusion coefficient. If the gas phase far from the drop is free of vapor, S_AG is defined by

$$S_\mathrm{AG} = \frac{2D_\mathrm{AG} M_\mathrm{A} p^0_\mathrm{A}(T_\infty)}{\rho_\mathrm{L} R T_\infty}\,. \tag{3}$$

Effect of a non-volatile additive

For the analysis of multicomponent droplet evaporation, the assumption that the droplet is spatially homogeneous is entirely reasonable due to the rapid rate of molecular diffusion within the droplet. This assumption may not be valid when high molecular weight additives or contaminants are present because of the low rate of diffusion of the additive. The concentration of a non-volatile additive, B, as a function of time and radial position in a droplet is given by

$$\frac{\partial C_\mathrm{B}}{\partial t} = \frac{1}{r^2}\frac{\partial}{\partial r}\left(r^2 D_\mathrm{AB}\frac{\partial C_\mathrm{B}}{\partial r}\right), \tag{4}$$

where C_B is the concentration of the additive and D_AB is the diffusivity of the additive in solvent A. Because the additive is not volatile, the flux through the surface of the drop is zero. Also, the flux at the center of the drop is zero due to symmetry. Thus, the boundary conditions are given by

$$\frac{\partial C_\mathrm{B}(0,t)}{\partial r} = \frac{\partial C_\mathrm{B}(a,t)}{\partial r} = 0\,. \tag{5}$$

The solvent concentration, C_A, is also governed by an equation of the form of Eq. (4), with the boundary condition at $r = 0$ given by Eq. (5), but in this case the boundary condition at the surface is

$$D_\mathrm{AB}\frac{\partial C_\mathrm{A}(a,t)}{\partial r} = -k_\mathrm{G}\frac{p^0_\mathrm{A}(T_\mathrm{a})}{RT_\mathrm{a}}\,, \tag{6}$$

where k_G is the gas-phase mass-transfer coefficient. If the surrounding gas is stagnant, $k_\mathrm{G} = D_\mathrm{AG}/a$, where D_AG is the diffusion coefficient of the solvent in the stagnant gas. If there is gas flow, k_G is a function of the Peclet number defined by $Pe = 2aU_\infty/D_{ij}$, where U_∞ is the gas velocity

upstream of the droplet. Taflin and Davis [13] and Zhang and Davis [14] measured mass-transfer coefficients as a function of the Peclet number for evaporating droplets. In the experiments described below, a small gas flow was used to remove vapor from the chamber to maintain $p_A(T_\infty) \sim 0$. For the low gas velocities and small droplets used in this study, the effect of the gas flow on the mass transfer was negligible.

Calculating the size change for a droplet containing a non-volatile additive is more complicated than for a pure-component droplet, and can be determined from

$$\frac{da}{dt} = \frac{a}{3\langle V_m \rangle}\frac{d\langle V_m \rangle}{dt} - \frac{\langle V_m \rangle D_{AB} p_{A,a}}{aRT}, \quad (7)$$

subject to the initial condition $a = a_0$ at $t = 0$. Here $p_{A,a}$ is the partial pressure of solvent at the droplet surface, and V_m is the mean molar volume given by $V_m = \sum x_i V_i$, where x_i and V_i are the mole fraction and molar volume of species i, respectively, and the summation is over all components in the droplet. The brackets, $\langle\ \rangle$, indicate a value averaged over the volume of the drop.

Equation (7) can be used to predict the evaporation rate of a droplet containing a non-volatile additive provided the partial pressure of the solvent at the surface of the drop, $p_{A,a}$, is known. For a pure component, $p_{A,a}$ is the vapor pressure of the material at the surface temperature. The partial pressure of component A in a homogeneous multicomponent mixture can be determined from $p_{A,a} = x_A \gamma_A p_A^0$, where γ_A is the activity coefficient of species A in the liquid. Unfortunately, for the system containing a solvent and a non-volatile additive, predicting the equilibrium partial pressure of the solvent can be more difficult due to the radially varying concentration within the droplet.

The evaporation rate experiments described here were conducted with a high molecular weight polymer in an organic solvent. The solvent partial pressure at the surface of the drop may be estimated from the Flory–Huggins theory. This theory, developed independently by Flory [15] and Huggins [16], is based on a lattice model of the solvent/polymer system. Using this model, the activity of the solvent is determined from

$$\ln a_s = \ln(1 - x_p V_p/V_m) + x_p V_p/V_m + \chi(x_p V_p/V_m)^2 . \quad (8)$$

Here χ is the Flory–Huggins interaction parameter, and x_p and V_p are the mole fraction and molar volume of the polymer solute, respectively. The first two terms on the right-hand side of Eq. (8) are due to entropy changes that result upon mixing of solvent and polymer molecules, and the third term is enthalpic in nature.

The Flory–Huggins interaction parameter can be estimated from knowledge of the solubility parameters, δ_i, for the solvent and solute. Fried [17] suggests the relation

$$\chi = (V_s/RT)(\delta_s - \delta_p)^2 \quad (9)$$

for calculating χ; however, Prausnitz et al. [18] warn that Eq. (9) provides a good guide for qualitative considerations of polymer stability, but is less useful for quantitative studies. We used Eq. (9) for lack of better alternative.

Using the method of Small [19] and data published by Fedors [20], the solubility parameter for TEP was calculated to be $17.8 \times 10^3\ J^{1/2}\,m^{-3/2}$. Prausnitz et al. reported a value of $19.4 \times 10^3\ J^{1/2}\,m^{-3/2}$ for the solubility parameter of PMMA. Using these values of the solubility parameters and Eq. (9), a value of $\chi = 0.176$ was calculated for the Flory–Huggins interaction parameter. Equation (8) can therefore be used to calculate the activity of triethyl phosphate at the surface of the drop as a function of PMMA concentration.

Experimental

Materials

Triethyl phosphate (99%) was obtained from Aldrich Chemical Company and used as the organic solvent in the evaporation experiments. Triethyl phosphate (TEP) has a molecular weight of 182.16 $g\,mol^{-1}$, a specific gravity of 1.072, and a refractive index of 1.4050. It was used without further purification. Poly(methyl methacrylate) (PMMA) was used for the non-volatile polymer additive. It was obtained from Rohm and Haas Company (Acryloid K-125, now called Paraloid K-125). The PMMA is a white powder with a specific gravity of 1.15, refractive index of 1.489, and a mean molecular weight of $\sim 4.5 \times 10^6\ g\,mol^{-1}$. The median particle size of the PMMA powder was 74 μm.

Equipment and techniques

Viscosity measurements of the PMMA/TEP solution were made with a Cannon–Fenske Routine Viscometer, and evaporation rate measurements were made using a temperature-controlled bihyperboloidal electrodynamic balance (EDB), shown in Fig. 1. The EDB uses superimposed a.c. and d.c. electric fields to levitate a charged particle in the path of a laser beam. A 10 mW He–Ne laser was used for elastic-scattering measurements.

Two light-scattering methods were applied to size the droplets. A 512 element photodiode array (PDA) mounted on the ring electrode recorded the intensity of scattered light as a function of scattering angle θ, where θ is measured from the direction of propagation of the laser beam.

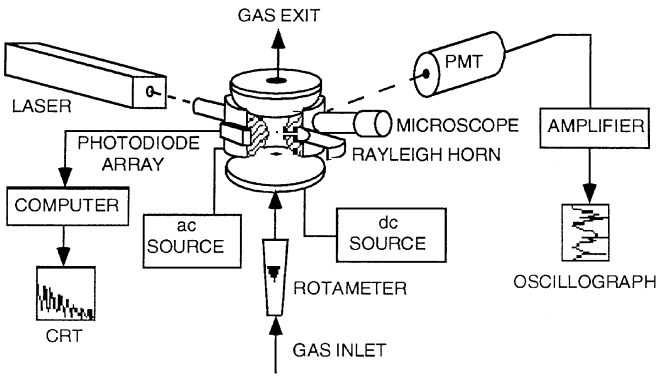

Fig. 1 A schematic of the bihyperboloidal electrodynamic balance used for the microdroplet evaporation experiments

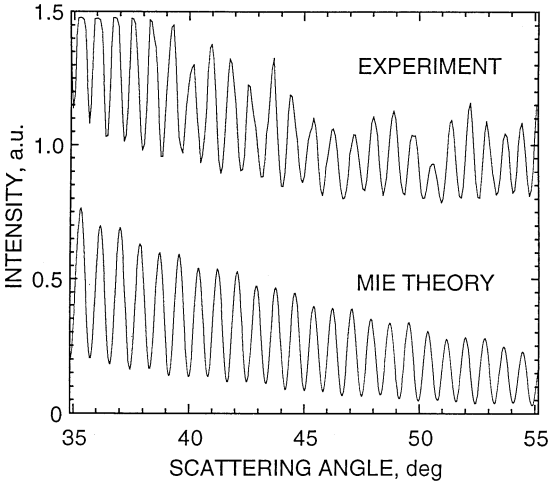

Fig. 2 Experimental and computed phase functions obtained for a single levitated TEP droplet

These so-called phase functions were recorded using a PC and compared with Mie theory to determine the size at any particular instant. A photomultiplier tube (PMT) mounted at right angle to the laser beam was used to record the morphology dependent resonance spectrum. The resonance spectrum results from internal reflection and refraction of the light wave that lead to constructive and destructive interference. It has been shown that the size and refractive index can be determined to about one part in 10^5 [21] by comparing experimental resonance spectra with Mie theory [22]. Examples of phase functions and resonance spectra are presented in Figs. 2 and 3, respectively. The experimental results are compared with Mie theory in both figures.

To levitate a particle in the EDB, a d.c. potential is applied across the top and bottom electrodes to balance any vertical forces on the particle, such as fluid mechanical

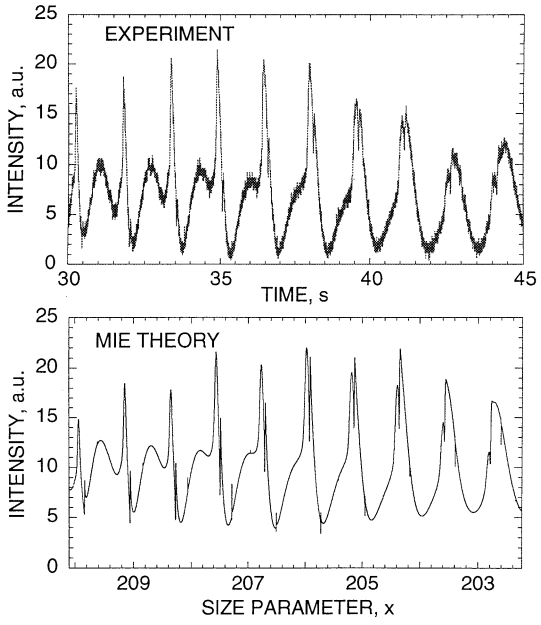

Fig. 3 An experimental resonance spectrum collected during the evaporation of a TEP microdroplet compared with a resonance spectrum computed using Mie theory

drag and gravity. An a.c. potential ($\sim$1000 V and $\sim$100 kHz) applied to the ring electrode provides a radial restoring force to the droplet to keep it centered in the balance. The droplet was injected through a hole in the top electrode by applying a high-voltage pulse ($\sim$5 kV) to a microliter syringe with a small amount of the liquid on the tip. A similar hole in the bottom electrode was used to introduce gas flow into the chamber. Oil pumped from a constant-temperature bath was circulated through the hollow top and bottom electrodes to maintain temperature control. Viewing ports in the ring electrode allowed the laser beam to enter and exit, the particle to be viewed, and phase functions and resonance spectra to be collected.

A second EDB was used to measure the extremely small change in size associated with the residual microdroplet at later times in the evaporation process. This device was a double-ring electrodynamic balance coupled to a Raman spectrometer as shown in Fig. 4. The double-ring configuration allows a large collection angle for light-scattering measurements, a feature that is crucial for spectroscopic studies. A 5 W argon-ion laser was used to illuminate the particle from below, and a SPEX 1403 0.85 m double monochromator collected the inelastically scattered light at $\theta = 90^\circ$ and $\phi = 90^\circ$. The detector was a 600-channel optical multichannel analyzer (OMA).

After sufficient time elapsed for most of the solvent to evaporate from the levitated droplet, a small spherical drop composed primarily of polymer remained. The final

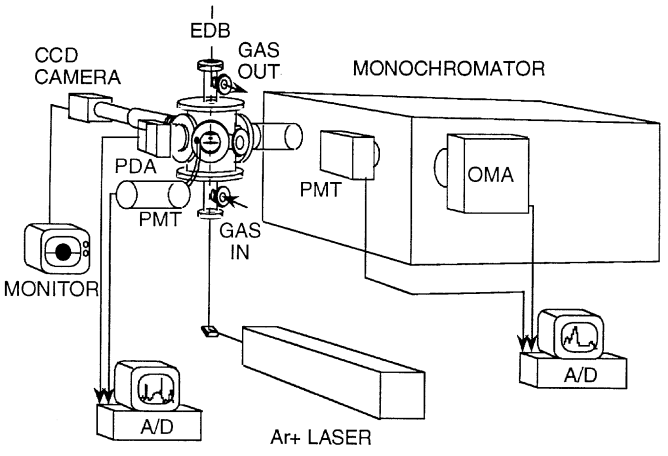

Fig. 4 The double-ring electrodynamic balance system used for the Raman spectroscopy measurements

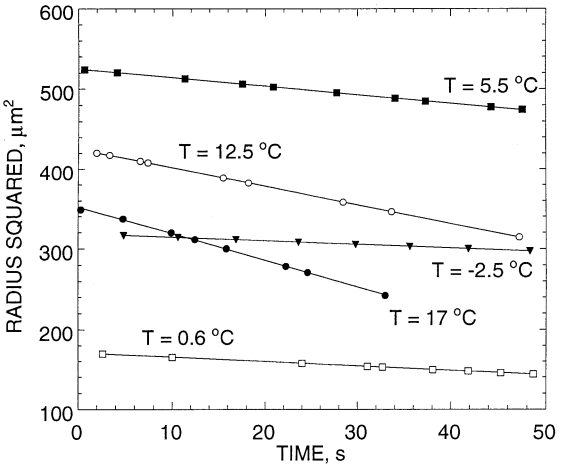

Fig. 5 The radius squared versus time during the evaporation of TEP droplets at various temperatures

evaporation rate of the droplets, indicative of the rate at which solvent molecules diffuse through the polymer matrix, was measured using output resonances that were superimposed upon Raman peaks corresponding to stretching and vibrational modes of C–H bonds. Just as the incident light from the laser beam can undergo resonance within the microdroplet, the inelastically scattered light can resonate within the drop. When this occurs, an additional peak can be observed on existing Raman peaks in the spectrum. By monitoring the spectral location of these additional peaks, the size change of the microdroplet can be determined. In 1990, Schweiger reviewed applications of Raman spectroscopy to microparticle studies [24], and the reader is referred to that paper for additional details.

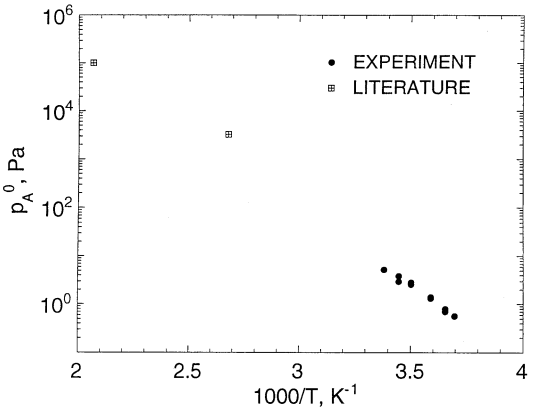

Fig. 6 Experimentally determined vapor pressures for TEP obtained from microdroplet levitation experiments

Results and discussion

Pure-component vapor pressures

The vapor pressure of triethyl phosphate was determined over a range of temperatures by measuring the evaporation rate of pure-component droplets and applying Eqs. (2) and (3). The size of the drop was determined by matching the experimental resonance spectrum to Mie theory, yielding the representative results shown in Fig. 3. Some of the evaporation data for TEP obtained in the temperature range 270.7–290.2 K are plotted as a^2 versus time in Fig. 5. To obtain the vapor pressure from the slopes of these graphs, it is necessary to estimate the gas-phase diffusion coefficient, D_{AG}. Gas-phase diffusivities were determined using the Wilke and Lee correlation presented by Reid et al. [25]. Figure 6 presents the vapor pressures determined in this way as a function of temperature. Also shown in the figure are two data points obtained from the literature which correspond to much higher temperatures than used here.

To explore the effect of the polymer additive, a small amount (0.76 wt%) of PMMA was added to triethyl phosphate and evaporation experiments were repeated. Graphs of a^2 versus time for two such experiments are presented in Fig. 7. The evaporation rates of the droplets containing the polymer are significantly lower than the pure component rates plotted in the figure. A solvent partial pressure of 4.36 Pa is consistent with the observed evaporation rates at smaller times, whereas the vapor pressure of pure TEP at the temperature of the experiments (297.2 K) is 6.41 Pa. The temperature would have to have been about 5 K lower to account for the reduced vapor pressure. The

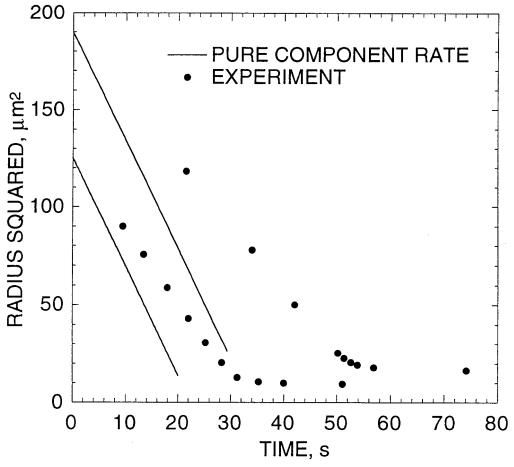

Fig. 7 A graph of the radius squared versus time for two microdroplets composed of TEP and PMMA

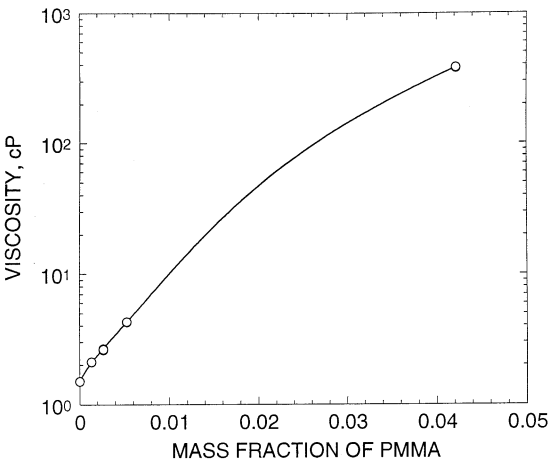

Fig. 8 The viscosity of the PMMA/TEP solution as a function of PMMA concentration

estimated error in the temperature measurements is about 0.2 K due to small fluctuations in the chamber temperature, so the reduced evaporation rate is not due to an error in the temperature measurement.

Figure 7 shows that there was a very substantial reduction in the evaporation rate after the droplet volume decreased to about 3% of the initial volume. The very small evaporation rates encountered at later times were measured using Raman data as described below.

Solute concentrations

To model the solute concentration with the evaporating microdroplet, Eqs. (4) and (5) were solved numerically using a finite-difference scheme in the radial direction and an implicit numerical differentiation formula (ODE15s, Matlab program by Mathworks Corp.) to advance in time. The solute concentration was assumed to be initially uniform throughout the droplet, and the solute was assumed to be non-volatile.

To model the initial evaporation of a microdroplet with the PMMA additive, it was necessary to estimate the liquid-phase diffusion coefficient, D_{AB}. This was accomplished by relating the diffusion coefficient to the viscosity using the relation

$$D_{AB} = D_0(\mu_0/\mu) \,, \tag{10}$$

where D_0 and μ_0 are the diffusion coefficient and viscosity at infinite dilution, respectively. This inverse dependence of the diffusivity with viscosity is consistent with many theoretical and semi-empirical correlations for liquid-phase diffusion coefficients.

The viscosities of PMMA/TEP solutions were measured as a function of polymer concentration, and the diffusion coefficient was empirically related to the PMMA concentration. Figure 8 shows the results of the viscosity measurements made at 297.0 K. To incorporate these measurements in the numerical model, a third-order polynomial was fit through the data. The least-squares fit resulted in the following relation between the viscosity and the PMMA concentration:

$$\mu(f_i) = 1.5117 + 417.76 f_i - 6557.2 f_i^2 + 4.934 \times 10^6 f_i^3 \,, \tag{11}$$

where the viscosity, μ, is in cP and f_i is the mass fraction of PMMA in solution.

The infinite dilution viscosity was determined by extrapolating the viscosity curve in Fig. 8 to zero-mass fraction. To estimate the infinite dilution diffusion coefficient, values for D_0 were obtained from the literature for systems of PMMA and various organic solvents. Brandrup and Immergut [25] report values for D_0 of 1.19×10^{-11}, 1.38×10^{-11} and $1.43 \times 10^{-11}\,m^2\,s^{-1}$ for PMMA/acetone, PMMA/tetrahydrofuran, and PMMA/*n*-butyl chloride at 293.2 K, respectively. They also reported $D_0 = 1.5 \times 10^{-11}\,m^2\,s^{-1}$ for *n*-butyl chloride at 307.7 K. Based on these values, we estimate the infinite dilution diffusion coefficient for the PMMA/TEP system to be $1.0 \times 10^{-11}\,m^2\,s^{-1}$ at 297.2 K.

The calculated concentration distributions of the polymer additive within the droplet during the first 2 s of evaporation are presented in Fig. 9. The calculations are based on the numerical solution of Eq. (4). The initial size used for the computations was $a_0 = 11.40\,\mu m$, and the initial concentration of PMMA was $1.95 \times 10^{-3}\,mol\,m^{-3}$.

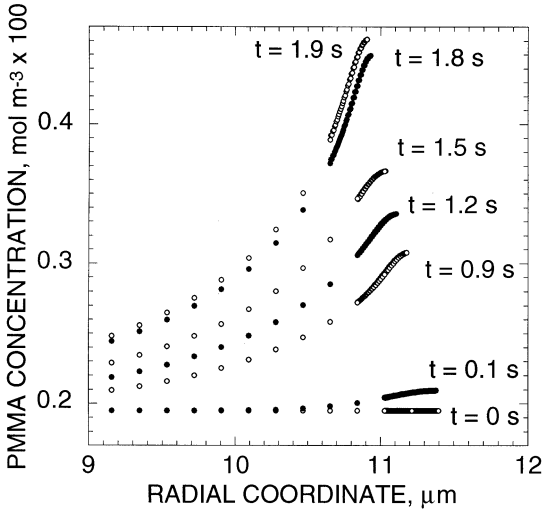

Fig. 9 The computed concentration of PMMA within the droplet at a temperature of 297.2 K for short times for an initial radius of 11.40 μm and for TEP partial pressures determined using the Flory–Huggins model

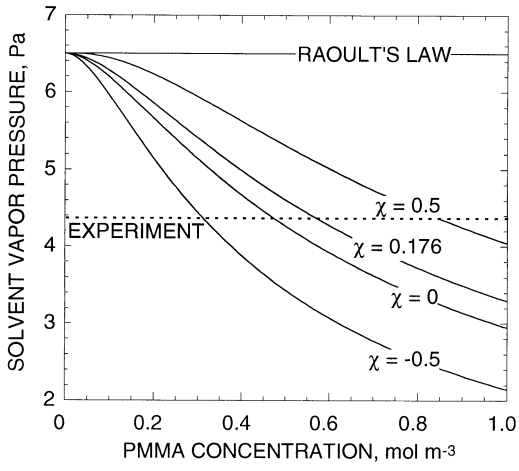

Fig. 10 The solvent vapor pressure at 297.2 K as a function of polymer concentration determined from Flory–Huggins theory. Different values of the Flory–Huggins interaction parameter, χ, are shown. The vapor pressure determined from Raoult's law, $p_{Aa} = x_A p_A^0$, is also shown

The temperature was 297.2 K. The computations indicate a rapid increase in the polymer concentration at the surface of the drop. The points shown in Fig. 9 correspond to the locations of the nodes in the numerical solution. A finer mesh was used near the interface to account for movement of the interface as the droplet evaporated. The PMMA concentration near the moving surface is difficult to model numerically [26], and it was not possible to model the droplet evaporation for long times due to the very steep concentration profiles that developed. Although the numerical model was not robust enough to obtain a^2 versus time results to compare with experimental data over the entire duration of an experiment, the short-time solution provides insight into the observed phenomena.

The a^2 versus time data in Fig. 7 are consistent with a constant partial pressure of the solvent during the early part of each experiment, whereas the bulk concentration of the polymer in the droplet increased dramatically as TEP evaporated. The constant evaporation rate suggests that the interfacial concentration of PMMA was constant. Furthermore, the data indicate a significant reduction in the solvent partial pressure compared with its pure-component vapor pressure, but the cause of this reduction is not clear. To explore this issue we calculated the vapor pressure of the solvent using Flory–Huggins theory, and the results are shown in Fig. 10 for several values of the Flory–Huggins interaction parameter. Also shown in the figure is the partial pressure of TEP determined from Raoult's law. For the low concentrations of PMMA during the early part of the evaporation process, the partial pressure reduction obtained using Raoult's law is negligible. The vapor pressure consistent with the measured evaporation rates at smaller times is also shown in the figure. It is apparent from Fig. 10 that the observed evaporation rate is not consistent with application of Raoult's law or Flory–Huggins theory. It is likely that some other interfacial phenomenon influences the evaporation rate. One possibility is that PMMA is surface-active in TEP. This could account for the constant evaporation rate observed at early times.

Raman measurements

As indicated above, after most of the TEP had evaporated, the evaporation rate was found to be extremely low. In this regime, the evaporation can be expected to be limited by the rate at which solvent molecules diffuse through the polymer matrix. To measure the very small size changes associated with the droplet evaporation rate near the end of an experiment, a droplet composed of PMMA and TEP was suspended in the double-ring EDB shown in Fig. 4, and Raman spectra were collected near a wave number shift of 2900 cm^{-1}, which corresponds to C–H stretching and vibrational modes. At certain combinations of size and refractive index the Raman-shifted light undergoes resonance in the droplet cavity, and the Raman signal is enhanced. A resonance associated with the Raman-shifted light is called an output resonance, whereas resonances of the incident light are called input resonances. Output resonances are much weaker than input resonances

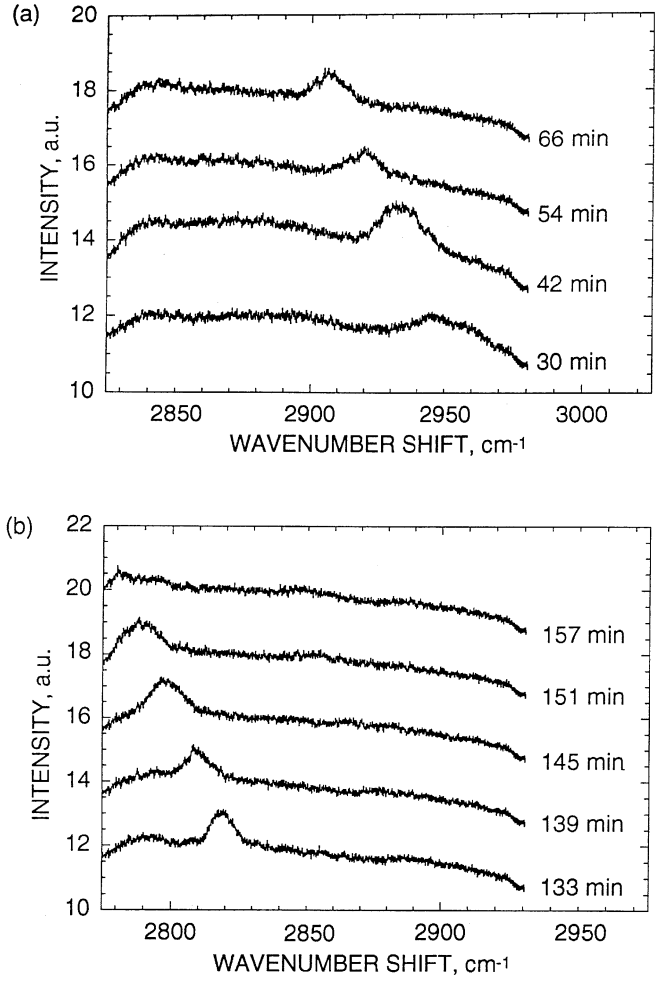

Fig. 11 The Raman spectra corresponding to the C–H bond used to measure the rate of droplet evaporation from the output resonances. Output resonances are shown in the spectra

because the intensity of Raman-shifted light is much less than that of the incident laser beam.

On resonance, the size parameter $X = 2\pi a/\lambda$ is constant, and can be used to determine the size change of the drop. The change in size is given by

$$\frac{da}{dt} = \frac{a}{\lambda}\frac{d\lambda}{dt} . \tag{12}$$

Here λ is the wavelength of the light resonating within the drop, which in the case of the output resonances is of lower energy than the incident light. The wavelength of the incident laser beam was 514.5 nm, and the wavelength of the Raman-scattered light was 605 nm.

Two examples of Raman spectra collected during the period of slow evaporation of a PMMA/TEP droplet are shown in Fig. 11. Note that as the droplet evaporates, the peak associated with the output resonance moves to lower wave number shift (higher energy). The rate at which this peak shifts was used to determine the size change of the drop. Because of the very small droplet size near the end of an experiment, it was not possible to obtain a precise size from the elastic scattering data. We estimated the drop diameter to be $\sim 2\ \mu$m based upon the image on the video monitor used to view the particles suspended in the EDB. With this estimate of the size, the evaporation rate determined from Eq. (12) is approximately $3 \times 10^{-6}\ \mu\mathrm{m\,s^{-1}}$. The evaporation rate, da/dt, given by Eq. (12) is a linear function of the radius, so an error in the drop radius leads to a corresponding error in the calculated evaporation rate.

In principle, one can determine the diffusion coefficient of solvent in the polymer by analysis of the mass loss at later times, but we have not attempted to model this process.

Summary

The effect of a high molecular weight polymer additive on the evaporation of TEP microdroplets was explored using an electrodynamic balance and light scattering techniques. Theoretical computations show that a high molecular weight additive or contaminant accumulates at the surface of the droplet as the solvent evaporates. Even at low concentrations, the PMMA reduces the evaporation rate of the droplet compared with the pure-component evaporation rate. The partial pressure of TEP appears to be constant during the early part of an experiment and is much lower than that predicted from conventional vapor/liquid thermodynamics. The experiments reported here suggest that PMMA is surface-active in TEP because of the reduced evaporation rate. After sufficient time has elapsed for the droplet to be composed primarily of polymer, the evaporation rate exhibits a large decrease that is likely governed by the rate at which solvent molecules diffuse through the polymer matrix. The size change in this regime was measured by observing the changes in the spectral location of output resonances in the Raman spectra.

Acknowledgements The authors express their gratitude to the U.S. Army CRDEC for primary financial support of this research, and to the National Science Foundation Grant Number CTS-9528897 for partial support. We would also like to express our appreciation to Professor John C. Berg for the use of the Cannon–Fenske viscometer.

References

1. Millikan RA (1911) Phys Rev Ser I 32:349
2. Davis EJ (1997) Aerosol Sci Tech 26:212
3. Taflin DC, Zhang SH, Allen TM, Davis EJ (1998) AIChE J 34:1310
4. Rubel GO (1981) J Colloid Interface Sci 81:188
5. Ravindran P, Davis EJ (1982) J Colloid Interface Sci 85:278
6. Rubel GO (1982) J Colloid Interface Sci 85:549
7. Rubel GO, Milham ME (1984) Chem Eng Sci 39:1043
8. Allen TM, Taflin DC, Davis EJ (1990) Ind Eng Chem Res 29:682
9. Buehler MF, Allen TM, Davis EJ (1991) J Colloid Interface Sci 146:79
10. Aardahl CL, Foss WR, Davis EJ (1996) Ind Eng Chem Res 35:2834
11. Widmann JF, Davis EJ (1997) Aerosol Sci Tech 27:243
12. Maxwell JC (1890) The Scientific Papers of Clerk Maxwell. Cambridge University Press, London
13. Taflin DC, Davis EJ (1987) Chem Eng Commun 55:199
14. Zhang SH, Davis EJ (1987) Chem Eng Commun 50:51
15. Flory PJ (1941) J Chem Phys 9:660
16. Huggins ML (1941) J Chem Phys 9:660
17. Fried JR (1995) Polymer Science and Technology. Prentice-Hall, Englewoods Cliffs, NJ
18. Prausnitz JM, Lichtenthaler RN, Gomes de Azevedo E (1986) Molecular Thermodynamics of Fluid-Phase Equilibria. Prentice-Hall, Englewoods Cliffs, NJ
19. Small PA (1953) J Appl Chem 3:71
20. Fedors RF (1974) Polym Eng Sci 14:147
21. Chylek P, Ramaswamy V, Ashkin A, Dziedzic JM (1983) Appl Opt 22:2302
22. Mie G (1908) Ann Phys 25:377
23. Schweiger G (1990) J Aerosol Sci 21:483
24. Reid RC, Prausnitz JM, Poling BE (1987) The Properties of Gases and Liquids. McGraw-Hill, New York
25. Brandrup J, Immergut EH (1989) Polymer Handbook. Wiley, New York
26. Finlayson BA (1992) Numerical Methods for Problems with Moving Fronts. Ravenna Park Publishing Inc, Seattle, WA